

Search for Cosmic Strings in the COSMOS Survey

J. L. Christiansen* and E. Albin

Department of Physics, California Polytechnic State University, San Luis Obispo, California 93407, USA

J. Goldman and I.P.W. Teng

Department of Physics, National University of Singapore, Singapore, 117542

M. Foley

Department of Biomedical Engineering, California Polytechnic State University, San Luis Obispo, California 93407, USA

G. F. Smoot

*Lawrence Berkeley National Laboratory, Space Sciences Laboratory
and Department of Physics, University of California, Berkeley, California 94720, USA*

(Dated: March 8, 2019)

We search the COSMOS survey for pairs of galaxies consistent with the gravitational lensing signature of a cosmic string. The COSMOS survey imaged 1.64 square degrees using the Advanced Camera for Surveys (ACS) aboard the Hubble Space Telescope (HST). Our technique includes estimates of the efficiency for finding the lensed galaxy pair. We find no evidence for cosmic strings with a mass per unit length of $G\mu/c^2 < 3.0 \times 10^{-7}$ out to redshifts greater than 0.6 at 95% confidence. This corresponds to a global limit on $\Omega_{strings} < 0.0017$.

PACS numbers: 98.80.Cq

I. INTRODUCTION:

Cosmic strings are topological defects that are likely to form during symmetry-breaking phase transitions in the early universe [1, 2]. Their well defined equations of motion and interaction potentials give us reason to believe that they have evolved into a modern day string network, observable through a variety of astrophysical phenomena [3]. More recently, cosmic superstrings have also been proposed in string theory models of inflation. These cosmic superstrings occur after the GUT scale transition and result in a stochastic network with interaction probabilities less than 1 [4]. In either case, the dimensionless scale of observational interest is $G\mu/c^2 \lesssim 10^{-6}$.

Although there has been considerable interest within the theory community, only a few observations bear on the subject: (1) cosmic microwave background (CMB), (2) gravitational waves, (3) gravitational lensing. The CMB power spectrum shows that cosmic strings are not the dominant factor in large-scale structure formation, although it is still possible that they contribute as much as 10% of the observed structure with strings $G\mu/c^2 \lesssim 0.7 \times 10^{-6}$ [5, 6]. Searches for individual strings in the CMB set a limit $G\mu/c^2 \lesssim 3.7 \times 10^{-6}$ [7]. These limits are expected to improve with the analysis of additional WMAP and Planck data sets [8, 9]. Bursts of gravitational waves are predicted from cusps in cosmic strings as they acquire a large Lorentz boost due to the string tension. A population of cusps and loops is expected to produce a stochastic background of gravita-

tional waves that can be detected via pulsar timing and also by direct measurement with LIGO [10–12]. The lack of a gravitational wave signal sets a limit on cosmic string masses that depends strongly on the reconnection probability of the string network. Limits as low as $G\mu/c^2 \lesssim 1.5 \times 10^{-8}$ have been reported. Gravitational lensing by a cosmic string of background galaxies has also been considered. Previously we searched the GOODS survey and concluded with 95% confidence that $G\mu/c^2 < 3.0 \times 10^{-7}$ out to redshifts greater than 0.5 and that $\Omega_{strings} < 0.02$ [13]. Our aim in this paper is to use the same technique to analyze the wider survey carried out by the COSMOS team with the Hubble Space Telescope (HST) Advanced Camera for Surveys (ACS). Since strings are linear objects and surveys increase by area we have found it necessary to perform the search in angular bins that improve the signal to noise.

In Section II we describe our data selection and present the correlation analysis used to search for cosmic strings in the COSMOS survey. We discuss the simulations needed to estimate the signal rates and detection efficiencies in Section III. These estimates are then used in Section IV to determine limits on individual cosmic strings as a function of mass and redshift as well as the global limit on the density of cosmic strings. Finally, we summarize our results in Sec. V.

II. DATA SAMPLE:

The COSMOS field is 1.64 degrees² centered on RA=10:00:28.6 and DEC=+02:12:21.0. Images were taken with the ACS aboard HST between July 2003 and June 2005 [14, 15]. We analyze the publicly available

*Electronic address: jlchrist@calpoly.edu

COSMOS Version 1.3 data in the F814W (I-band) filter which consists of 81 drizzled tiles with a resolution of $0.05''/\text{pixel}$. We apply a fiducial cut and use the central 1.57 degrees^2 of the survey.

A. Source identification

We use SExtractor version 2.5.0 (Source Extractor) to identify sources in the COSMOS survey [16, 17] following the *Hot* procedure outlined in [18]. For shape-sensitive analyses like weak lensing, Leauthaud et al. advocate a *Hot-Cold* method applied to un-rotated, undrizzled images. We validate our *Hot* catalogs against the public release of the well-understood Leauthaud et al. catalog containing 1.2 million objects which we refer to as the *LC2* catalog described in [18]. We do not perform a catalog-level search using the *LC2* catalog directly due to the difficulties in estimating the efficiency of finding lensed galaxies without access to the original COSMOS fits images and processing pipeline.

Several minor modifications need to be applied to Leauthaud’s *Hot* parameters [18] to account for the difference in resolution for the publicly available tiles. We set the `PIXEL_SCALE` to 0.5 arcsec, use a gaussian filter width of 2.5 pixels, and set the `DETECT_MINAREA` to 9 contiguous pixels above threshold. We also scale the apertures to 12 pixels, `PHOT_APERTURES` and `PHOT_AUTOAPERS`. Finally, to reduce the deblending slightly, we set the `DEBLEND_NTHRESH` to 32 and the `DEBLEND_MINCONT` to 0.1. The resulting catalog contains 812,463 objects with magnitudes brighter than 26.5.

B. Resolved galaxy selection

We select the resolved galaxies from this sample using the correlation of the peak surface brightness, `MU_MAX`, with the objects magnitude, `MAG_AUTO`. Figure 1 shows three regions of interest in the `MU_MAX` vs `MAG_AUTO` plane: resolved galaxies, point sources including stars, and spurious detections where the objects are too small to be consistent with the point spread function. There are 761,370 resolved galaxies, 36,823 point sources, and 14,270 spurious detections. The *LC2* catalog contains fewer spurious detections due to a prior cleaning procedure that included merging of small objects with nearby objects from the *Cold* catalog and removal of objects in regions of elevated noise that occur on the borders of the un-rotated tiles as well as near bright stars. To reproduce the additional “by hand” cleaning, we correlate our resolved galaxies with the *LC2* catalog.

We find that 96.4% of the resolved galaxies with magnitudes brighter than 23^{rd} magnitude are also found in the *LC2* catalog. Our magnitudes generally agree, but have a tail down to smaller values which we attribute to over deblending of larger objects. The 3.6% of events that don’t have a counterpart in the *LC2* catalog are all

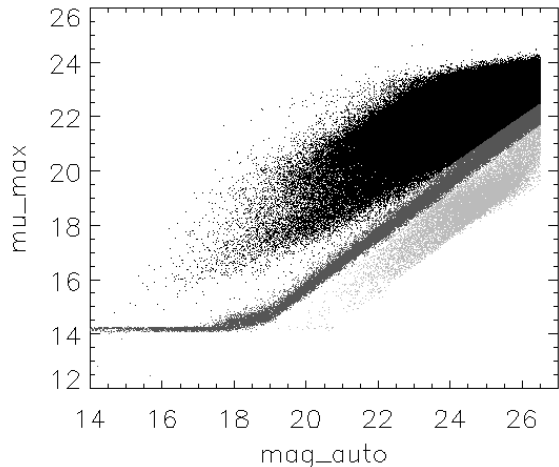


FIG. 1: Resolved galaxies (black points) are a distinct population. Also shown are point sources (dark gray) including stars, and spurious objects (light gray) that are too small to be consistent with the PSF.

found in the diffraction trails of very bright stars or in a few cases near the edge of the survey consistent with the more aggressive cleaning. The situation is understandably slightly worse for dimmer objects; 87.7% of the galaxies at 25^{th} magnitude have a counterpart in the *LC2* catalog. The magnitudes tend to agree well. The 12.3% of galaxies that don’t have a counterpart in the *LC2* catalog are again in fiducial regions that were removed by hand. Most of the rest are in regions with elevated noise. Very few appear to be legitimate detections.

To reproduce the cleaning as much as possible, we remove resolved sources in our catalog that are not included in the *LC2* catalog. This removes about 11.6% of our resolved galaxies. Any inefficiency that comes about from this requirement is included in our efficiency estimate. More importantly, though, this requirement protects us from overestimating the cosmic string lensing rate due to spurious detections.

We post-process our resolved galaxy catalog to identify the pixels in the image associated with each galaxy. The first step is to define a small but encompassing search region about each galaxy centroid. The second step is to find a bright pixel near the galaxy centroid. We then look for neighboring pixels that are 1σ above the noise threshold in the search region and attach them to the centroid pixel cluster. By iteratively connecting neighbors that are above the noise threshold, we eventually get a cluster of pixels that we identify as the galaxy. This process sometimes merges neighboring galaxies. In the event that a cluster of pixels reaches the edge of the search region or that two galaxies merge, we raise the neighbor threshold to 2σ and repeat the process until each galaxy is completely contained within the search region and does not contain the centroid from any other galaxy in the cata-

log. For a few very dim sources, the threshold is raised so high that there are no pixels left in the cluster and we remove these galaxies from the sample. This procedure cuts 0.15% of the sources. After selecting resolved galaxies also identified in the *LC2* catalog and identifying the pixel ID, the resulting catalogs contain 662,765 resolved galaxies.

C. Matched galaxy pair selection

To calculate the morphological similarity between each pair of galaxies we rely on the correlation and cross-correlation of the two galaxy images as we did previously in the GOODS search [13]. We first align the centroids and then calculate the correlation (*CORR*) and the cross-correlation (*XCORR*) of the pixels.

$$CORR = \frac{\sum I_1(x_i, y_i)^2 - \sum I_2(x_i, y_i)^2}{\sum I_1(x_i, y_i)^2 + \sum I_2(x_i, y_i)^2} \quad (1)$$

$$XCORR = \frac{2 \sum I_1(x_i, y_i) * I_2(x_i, y_i)}{\sum I_1(x_i, y_i)^2 + \sum I_2(x_i, y_i)^2} \quad (2)$$

where $I(x_i, y_i)$ is the intensity of each pixel in a galaxy and the subscript 1 or 2 refers to the galaxies being correlated. Galaxies with *CORR* near a value of zero have very similar magnitudes and galaxies with *XCORR* near a value of one are similar in shape. We define matched galaxy pairs as those within the ellipse defined by

$$\sqrt{(2 * CORR)^2 + (1 - XCORR)^2} < 0.29 \quad (3)$$

This cut was optimized on simulated lensing events and is slightly looser than the one used in our previous GOODS search.

In this analysis, we consider pairs of galaxies with opening angles, $\Delta\theta < 15''$. There are 96,413 matched pairs out of 7,081,011 total pairings with $\Delta\theta < 15''$ in the COSMOS survey.

D. Pairs distribution

The binned distribution of matched galaxy pairs is shown in Fig. 2. The distribution is divided into 4 overlapping angular bins: $-5^\circ:50^\circ$, $40^\circ:95^\circ$, $85^\circ:140^\circ$, and $130^\circ:185^\circ$. These bins are needed to reduce the background as the survey gets large. Because cosmic strings are linear objects, the signal scales with the width of the survey whereas the background scales with the area of the survey.

The orientation of each pair is defined by the location of the two galaxy centroids forming the pair. The string is presumed to pass between the galaxies at an angle perpendicular to the pair orientation. The angular bins therefore, correspond to a range of string angles on the

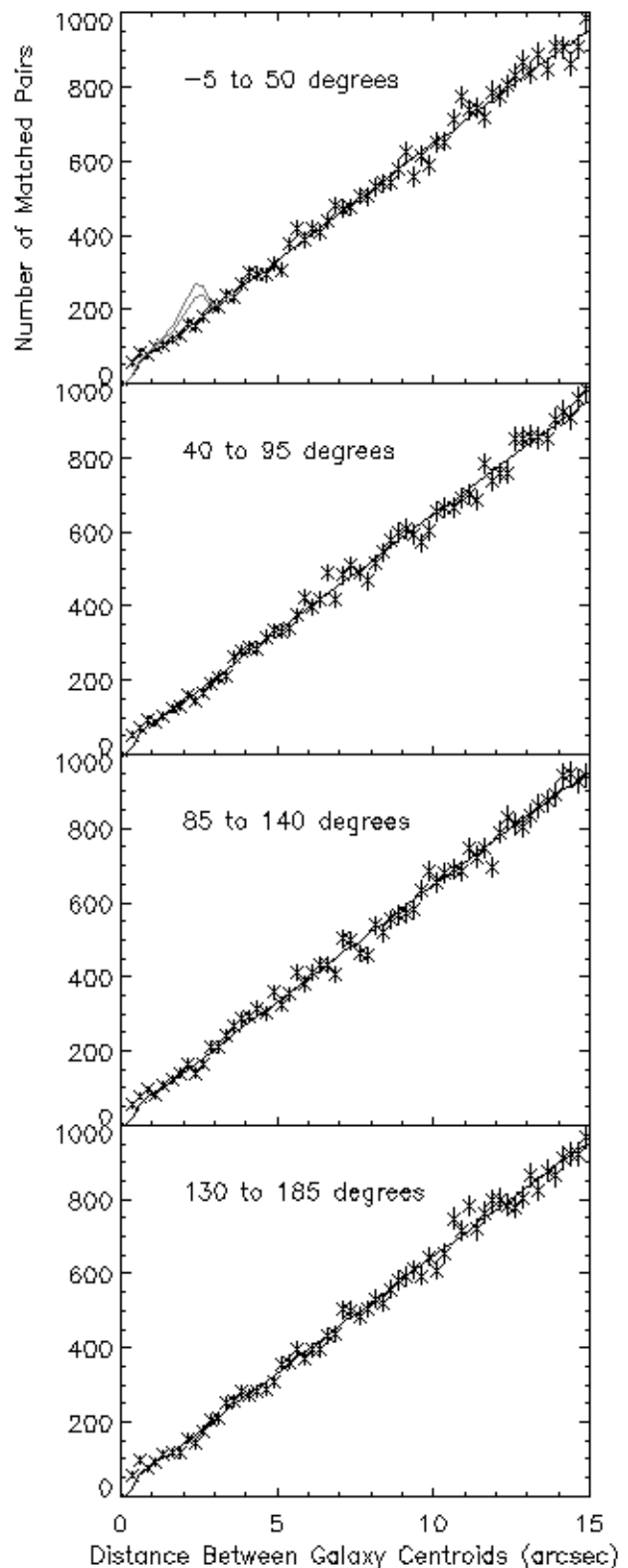


FIG. 2: Pairs of galaxies in four angular bins (points) are compared to background (solid line). The top panel shows one example of a simulated string (grey). The upper simulated string is the total number of pairs expected from the simulation with string length of 1.19° , redshift of 0.5, and $\delta \sin \beta$ of $4''$. The lower simulated string includes measurement inefficiencies.

sky. The overlap accounts for the resolution in the reconstructed angle and assures us that we are searching efficiently.

The background shape is characterized by the distribution of all pairs of galaxies regardless of size and shape. Because strings with masses large enough to create opening angles greater than $7''$ have been ruled out [7, 19], we normalize the background distribution to the number of measured matched pairs between $7''$ and $15''$. This gives us a reliable estimate of the background at smaller opening angles. From the background, we observe that SExtractor merges galaxies with opening angles smaller than $0.4''$.

In our signal region, between $0.4''$ and $7''$, the χ^2/dof of the matched pairs to the background is 0.99, 1.1, 1.3, and 1.4 for the four angular bins respectively. Based on the scaled background distribution, we report no evidence for an excess of pairs at small opening angles. Although there is no statistically significant excess in our signal region, we note that there is a small excess of signal below $1''$ and that the first data point in the signal region is systematically high. This excess is consistent with the fact that smaller galaxies tend to pass the correlation cuts more easily than larger galaxies. To investigate this region more carefully, we surveyed matched pairs with opening angles less than $1''$ by hand. We find that matched pairs tend to be discovered in regions of high galaxy density and that these regions tend to have other lensing candidates at the fairly high rate of $0.5/1'$. A full statistical analysis of these pairs shows no evidence of lensing and gives us a calibration curve for the background in high density regions.

III. COSMIC STRING SIMULATIONS:

Simulations are used to estimate both the number of lensed galaxy pairs based on the local density of galaxies and the efficiency of finding those pairs. The simulation of lensed galaxy pairs is the same as used previously in our GOODS search [13]. The idea is to use the density of galaxies in our catalog of sources to monte carlo the number of pairs that would exist from any theoretical string crossing our survey. The advantage of a catalog-level signal simulation is that we can quickly embed as many strings as needed to get an accurate estimate of the average number of lensed galaxies observed from a particular set of string parameters, including redshift and $\delta \sin \beta$. An example of the result from this simulation is shown in the top panel of Fig. 2.

Fig. 3 summarizes the efficiencies as a function of the opening angle between the galaxies and the string redshift. These efficiencies were estimated by embedding galaxies as realistically as possible into COSMOS tiles and then processing the modified tiles back through our analysis chain to see how many embedded sources are found. The curves include both the efficiency of identifying the embedded galaxies with SExtractor and the

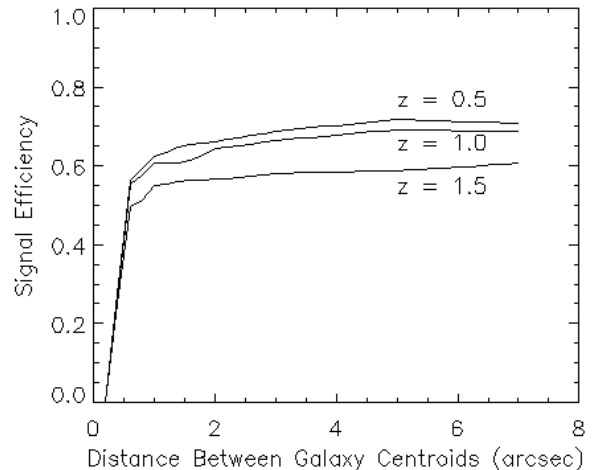


FIG. 3: Efficiency of detecting pairs of galaxies lensed by a cosmic string as a function of pair opening angle and redshift.

correlation and cross correlation selection cuts. Below $0.4''$ galaxies are merged by SExtractor and the pair is lost. For dim galaxies, which tend to have higher redshifts, noise in the galaxy detection becomes an increasingly important effect.

IV. RESULTS:

The distribution of matched galaxy pairs shown in Fig. 2 rises nearly linearly as expected. For comparison, pairs from a cosmic string at a redshift of 0.5 and $\delta \sin \beta$ of $4''$ are included on the plot and are normalized to the mean string length of 1.19° . The upper curve is the simulated signal without detection inefficiencies. The lower curve includes the measurement inefficiencies from Fig. 3.

We compare a wide variety of predicted cosmic string signals to the data to determine limits. The resulting 95% confidence limits are shown in Fig. 4. All four angular bins yield similar limits that extend from $1'' < \delta \sin \beta < 7''$. We average the four angular bins for the global limit. Taking the mean tilt of a string with respect to the observer to be $\langle \sin \beta \rangle = 2/\pi$ we relate the opening angle to the mass scale via the factor $8\pi \frac{G\mu}{c^2} = \delta \langle \sin \beta \rangle$ shown on the right-hand axis. We see no evidence for cosmic strings out to a redshift greater than 0.5 and place a limit on $G\mu/c^2 < 3.0 \times 10^{-7}$ at 95% C.L.

We combine the angular limits and use the average to set limits on the string density. If strings are rare occurrences, it is possible that none would appear in the COSMOS field and that other survey fields may yield different results. We can interpret our result, however, as excluding the possibility that 3 strings would be located in the field of view with 95% confidence. This corresponds to a

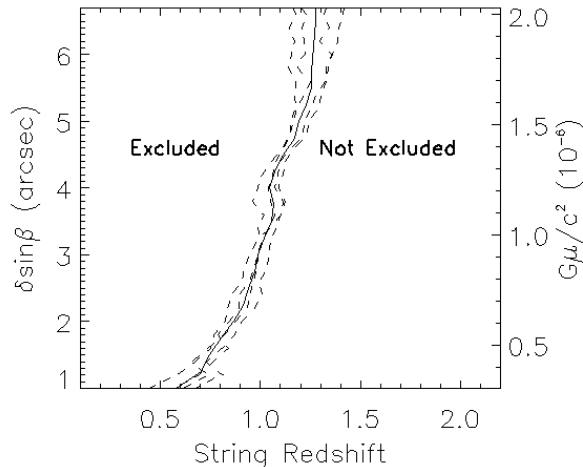


FIG. 4: Confidence limits at 95% for lensed galaxies produced by a cosmic string as a function of the string mass and redshift. Dashed lines are the individual limits from each angular bin shown above. The solid line is the average limit for all directions.

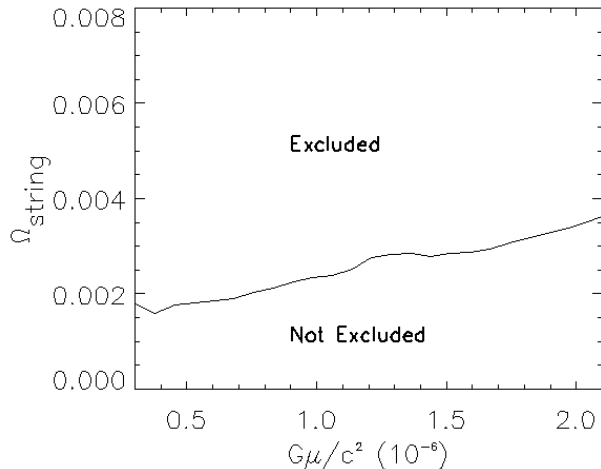


FIG. 5: Confidence limits at 95% on Ω_{string} as a function of the string mass.

string density

$$\Omega_{strings} \simeq \frac{N\mu}{fov \eta^2/3} \times \frac{8\pi G}{3H_0^2} \quad (4)$$

where $N = 3$ strings, μ is the mass per length of the string, fov is the survey field of view (1.57 square degrees) and η is the comoving distance computed with $h = 0.7$, $\Omega_M = 0.27$, and $\Omega_\Lambda = 0.73$. Figure 5 shows the string densities excluded by this method. The limit excludes a string density that is 0.17% of the critical density for the smallest mass strings and twice that for more massive strings.

V. CONCLUSION:

We use the COSMOS survey field to search for cosmic strings. We find no evidence for the existence of the gravitational lensing signature. We have included the observational efficiencies in our analysis using the same technique we used on the GOODS survey. Our results are summarized in Figs. 4 and 5. From this search we conclude with 95% confidence that $G\mu/c^2 < 3.0 \times 10^{-7}$ out to redshifts greater than 0.6 and that $\Omega_{strings} < 0.0017$. We note that these results are for long straight strings, but also exclude moderately curved strings.

The global limit on Ω_{string} is more than 10 times stronger than our previously published limit [13]. Our excluded masses are smaller than those excluded by other direct CMB searches [7, 20] but are larger than those reported by parameter fits to the CMB [21] as well as gravitational wave searches [10, 22]. We want to emphasize the complementary nature of these results, however. They are weaker in total, but search directly for strings that are small enough to be missed by other searches. They are also not sensitive to modeling parameters that may affect other searches and are therefore important confirmation of other results.

VI. ACKNOWLEDGEMENTS:

We would like to thank Kevin James and Timothy Fletcher for their early participation in this analysis project. We also thank Alexie Leauthaud for useful discussions of the COSMOS dataset and her catalog. This research used resources of the National Energy Research Scientific Computing Center, which is supported by the Office of Science of the U.S. Department of Energy under Contract No. DE-AC02-05CH11231.

-
- [1] T. Kibble, J. Phys. A **9**, 1387 (1976).
 - [2] J. Polchinski, hep-th/0412244.
 - [3] M. Hindmarsh and T. Kibble, Rep. Prog. Phys. **58**, 477 (1995).
 - [4] M. Sakellariadou, hep-th/0602276.

- [5] N. Bevis, M. Hindmarsh, M. Kunz, and J. Urrestilla, Phys.Rev. **D75**, 065015 (2007).
- [6] N. Bevis, M. Hindmarsh, M. Kunz, and J. Urrestilla, Phys.Rev.Lett **100**, 021301 (2008).
- [7] E. Jeong and G. Smoot, Astrophys. J. **624**, 21 (2005).

- [8] E. Jeong, C. Baccigalupi, and G. Smoot, arXiv:1004.1046.
- [9] N. Bevis, M. Hindmarsh, M. Kunz, and J. Urrestilla, arXiv:1005.2663v1.
- [10] F. Jenet et al., *Astrophys. J.* **653**, 1571 (2006).
- [11] B. Abbott et al., *Phys. Rev.* **D80**, 062002 (2009).
- [12] B. Abbott et al., *Nature* **460**, 990 (2009).
- [13] J. L. Christiansen et al., *Phys.Rev.* **D77**, 123509 (2008).
- [14] N. Scoville et al. (2007).
- [15] A. Koekemoer et al., *ApJS* **172**, 196 (2007).
- [16] E. Bertin, *SExtractor v2.4 user's manual* (2005).
- [17] E. Bertin and Arnouts, *Astron. and Astron. Suppl. Ser.* **117**, 393 (1996).
- [18] A. Leauthaud et al., *ApJS* **172**, 219 (2007).
- [19] L. Pogosian, S. Tye, I. Wasserman, and M. Wyman, *Phys. Rev.* **D68**, 023506 (2003).
- [20] A. Lo and E. Wright, astro-ph/0503120.
- [21] M. Wyman, L. Pogosian, and I. Wasserman, *Phys.Rev.* **D73**, 089905 (2006).
- [22] X. Siemens, V. Mandic, and J. Creighton, *Phys. Rev. Lett.* **98**, 111101 (2007).